**Journal of Engineering Mathematics manuscript No.**
(will be inserted by the editor)

# Effect of double fibre-reinforcement on localized bulging of an inflated cylindrical tube of arbitrary thickness

**Juan Wang · Yibin Fu**

Received: date / Accepted: date

**Abstract** We consider localized bulging of an inflated cylindrical hyperelastic tube of arbitrary thickness that is helically reinforced by two families of fibres. It is shown that localized bulging may become impossible, irrespective of the end conditions, when the tube wall becomes thick enough. This is in sharp contrast with an isotropic hyperelastic tube without fibre-reinforcement for which localized bulging has previously been shown to be possible no matter how thick the tube wall is and for which the membrane theory provides a very good approximation for wall-thickness/radius ratio as large as 0.67. Our findings provide a feasible explanation on why aneurysms cannot occur in healthy arteries but become possible following pathological changes. They can also be used to guide the design of tubular structures where localized bulging should be prevented.

**Keywords** Localized bulging · rubber tubes · aneurysm · fibre-reinforcement · nonlinear elasticity.

## 1 Introduction

It is well-known that a localized bulge will appear in an inflated tubular balloon when the internal pressure reaches a certain critical value. This phenomenon was examined more than a century ago by Mallock [1] who showed that the inflation pressure has a maximum even though the material is described by a linear constitutive law. This implies that localized bulging is due to geometrical softening, rather than material softening. This behaviour was commonly believed to be associated with the fact that in uniform inflation the pressure against volume has an $N$ shape in which the pressure has both a maximum and a minimum. Interestingly, when commonly used constitutive models for arteries are used to plot the pressure against volume in uniform inflation, it is found that the behaviour is monotonic. This fact forms the basis for the prevalent belief that aneurysm initiation cannot be a mechanical phenomenon – it is a purely biological process. However, recent studies have shown that the correspondence between the maximum pressure in uniform inflation and initiation pressure for localized bulging only exists when the resultant axial force is

Juan Wang
College of Science, University of Shanghai for Science and Technology, Shanghai 200093, China
E-mail: jwang@usst.edu.cn

Yibin Fu
School of Computing and Mathematics, Keele University, Staffordshire ST5 5BG, UK
E-mail: y.fu@keele.ac.uk

fixed during inflation, which is the case if the movement of one end of the tube is unrestricted. When it is the axial length that is fixed, which is the case for arteries, localized bulging may be possible even if the pressure is monotonic in uniform inflation. We refer to Fu *et al* [2] and Fu & Ilichev [3] for a review of the relevant literature.

If aneurysm initiation in pathological arteries is accepted as a mechanical bifurcation phenomenon, an explanation must also be found for the fact that aneurysms should not occur in healthy arteries. One such explanation is offered in this paper: it is shown that under double fibre-reinforcement localized bulging may become impossible if the wall thickness is large enough, with the threshold wall thickness depending on the strength and orientation of fibre-reinforcement. The latter dependence also accommodates the possibility that under some pathological changes localized bulging can still occur. This realization may have applications in other situations where aneurysm prevention is desired. One such situation is the Anaconda wave energy extraction device which essentially consists of a rubber tube filled with water which is placed in the sea. It is continuously squeezed or enlarged locally by the surrounding water causing pressure waves along its length. The distensible tube must be designed to have structural integrity and to have the correct distensibility so that the bulge wave speed matches the incident wave speed without aneurysm formation; see Bucchi & Hearn [4].

Our present study is part of a systematic research program devoted to an improved understanding of the localized bulging phenomenon in inflated cylindrical tubes, and is the second paper in the series that examines the effects of bending stiffness after Fu *et al* [5]. It compliments previous studies on the so-called limiting point instability which refers to the existence of a pressure maximum in uniform inflation. This instability was studied by Alexander [6], Benedict *et al* [7] and Caroll [8] for isotropic membrane tubes, and by Kanner & Horgan [9] and Horny *et al* [10] for fibre-reinforced membrane tubes. The effect of finite thickness on this type of instability was first examined by Ren *et al* [11] who showed that there exists a critical thickness above which the limiting point instability becomes impossible. However, as mentioned earlier, this type of instability is relevant to localized bulging only when the resultant axial force is fixed during inflation.

The rest of this paper is organized as follows. In the next section we formulate the problem and derive the bifurcation condition for localized bulging. Numerical results are then presented in Section 3. The paper is concluded in Section 4 with a summary and some additional remarks.

## 2 Governing equations

We are concerned with axi-symmetric deformations of a hyperelastic cylindrical tube that initially has inner radius $A$ and outer radius $B$. In terms of cylindrical polar coordinates, the position vector in the undeformed and current configurations are given by

$$\boldsymbol{X} = R\boldsymbol{e}_r + Z\boldsymbol{e}_z, \quad \boldsymbol{x} = r(R,Z)\boldsymbol{e}_r + z(R,Z)\boldsymbol{e}_z, \tag{2.1}$$

respectively, where the unit vectors $\boldsymbol{e}_r$ and $\boldsymbol{e}_z$ denote the usual basis vectors, and we have indicated the fact that the Eulerian polar coordinates $r$ and $z$ are functions of $R$ and $Z$ only. Since the deformation is axially symmetric, the kinematics of each surface $R = \text{const}$ in the undeformed configuration is the same as that of a membrane examined in many previous studies, and so the principal directions of stretch coincide with the lines of latitude, the meridian and the normal to the deformed surface. Denoting the unit vectors in these principal directions by $\boldsymbol{e}_1, \boldsymbol{e}_2, \boldsymbol{e}_3$, respectively, we have

$$\boldsymbol{e}_1 = \boldsymbol{e}_\theta, \quad \boldsymbol{e}_2 = \cos\gamma\boldsymbol{e}_z + \sin\gamma\boldsymbol{e}_r, \quad \boldsymbol{e}_3 = -\sin\gamma\boldsymbol{e}_z + \cos\gamma\boldsymbol{e}_r, \tag{2.2}$$

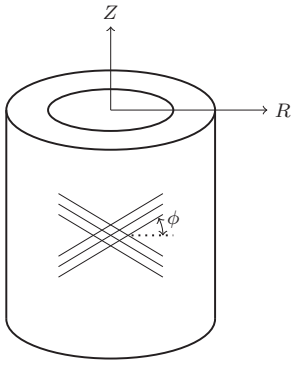


**Fig. 1** Geometry of a helically fibre-reinforced cylindrical tube

where $\gamma$ is the angle between the meridian and the $z$-direction in the deformed configuration and is now dependent on $R$. The associated principal stretches are given by

$$\lambda_1 = \frac{r}{R}, \qquad \lambda_2 = \sqrt{r'^2 + z'^2}, \qquad \lambda_3 = 1/(\lambda_1\lambda_2), \tag{2.3}$$

where a prime denotes partial differentiation with respect to $Z$, and the incompressibility condition has been used to write down the expression for $\lambda_3$. As expected, for each fixed $R$, these expressions are formally the same as those for a membrane tube.

We assume that the cylindrical tube is reinforced helically by two symmetric families of fibres; see Fig.1. With incompressibility assumed, the strain energy function $\Psi$ is then a function of the seven invariants $I_1, I_2, I_4, I_5, I_6, I_7, I_8$ defined by [12]

$$I_1 = \operatorname{tr} C, \quad I_2 = \frac{1}{2}(I_1^2 - \operatorname{tr} C^2), \quad I_4 = \boldsymbol{M}\cdot C\boldsymbol{M}, \quad I_5 = \boldsymbol{M}\cdot C^2\boldsymbol{M},$$
$$I_6 = \boldsymbol{M}'\cdot C\boldsymbol{M}', \quad I_7 = \boldsymbol{M}'\cdot C^2\boldsymbol{M}', \quad I_8 = \boldsymbol{M}\cdot C\boldsymbol{M}', \tag{2.4}$$

where $C$ is the right Cauchy-Green strain tensor, and $\boldsymbol{M}$ and $\boldsymbol{M}'$ are the directions of the two families of fibres in the reference configuration. The Cauchy stress tensor is then given by

$$\sigma = -pI + 2\Psi_1 B + 2\Psi_2(I_1 B - B^2) + 2\Psi_4 \boldsymbol{m}\otimes\boldsymbol{m}$$
$$+2\Psi_5(\boldsymbol{m}\otimes B\boldsymbol{m} + B\boldsymbol{m}\otimes\boldsymbol{m}) + 2\Psi_6 \boldsymbol{m}'\otimes\boldsymbol{m}'$$
$$+2\Psi_7(\boldsymbol{m}'\otimes B\boldsymbol{m}' + B\boldsymbol{m}'\otimes\boldsymbol{m}') + \Psi_8(\boldsymbol{m}\otimes\boldsymbol{m}' + \boldsymbol{m}'\otimes\boldsymbol{m}), \tag{2.5}$$

where $p$ is the pressure associated with the constraint of incompressibility, $B$ is the left Cauchy-Green strain tensor, $\Psi_i = \partial\Psi/\partial I_i$ $(i = 1, 2, \ldots, 8)$, and $\boldsymbol{m} = F\boldsymbol{M}$, $\boldsymbol{m}' = F\boldsymbol{M}'$ with $F$ being the deformation gradient.

In terms of the basis vectors, the two fibre directions may be written as

$$\boldsymbol{M} = \cos\phi\,\boldsymbol{e}_\theta + \sin\phi\,\boldsymbol{e}_z, \quad \boldsymbol{M}' = \cos\phi\,\boldsymbol{e}_\theta - \sin\phi\,\boldsymbol{e}_z, \tag{2.6}$$

where $\phi$ is the constant angle between one family of fibres and the circumferential direction; see Fig.1. From the fact that $B = \lambda_1^2\boldsymbol{e}_1\otimes\boldsymbol{e}_1 + \lambda_2^2\boldsymbol{e}_2\otimes\boldsymbol{e}_2 + \lambda_3^2\boldsymbol{e}_3\otimes\boldsymbol{e}_3$ and $C = \lambda_1^2\boldsymbol{e}_\theta\otimes\boldsymbol{e}_\theta + \lambda_2^2\boldsymbol{e}_z\otimes\boldsymbol{e}_z + \lambda_3^2\boldsymbol{e}_r\otimes\boldsymbol{e}_r$, we may deduce that the deformation gradient $F$ takes the form

$$F = \lambda_1\boldsymbol{e}_1\otimes\boldsymbol{e}_\theta + \lambda_2\boldsymbol{e}_2\otimes\boldsymbol{e}_z + \lambda_3\boldsymbol{e}_3\otimes\boldsymbol{e}_r. \tag{2.7}$$

It then follows that

$$\boldsymbol{m} = F\boldsymbol{M} = \lambda_1 \cos\phi\, \boldsymbol{e}_1 + \lambda_2 \sin\phi\, \boldsymbol{e}_2, \quad \boldsymbol{m}' = F\boldsymbol{M}' = \lambda_1 \cos\phi\, \boldsymbol{e}_1 - \lambda_2 \sin\phi\, \boldsymbol{e}_2, \tag{2.8}$$

and so

$$I_4 = \boldsymbol{m} \cdot \boldsymbol{m} = \lambda_1^2 \cos^2\phi + \lambda_2^2 \sin^2\phi = I_6, \tag{2.9}$$

$$I_5 = \boldsymbol{m} \cdot B\boldsymbol{m} = \lambda_1^4 \cos^2\phi + \lambda_2^4 \sin^2\phi = I_7. \tag{2.10}$$

We make the further assumption that the two families of fibres are mechanically equivalent and so the strain energy remains invariant when $I_4$ and $I_6$ are interchanged. This implies that $\Psi_4 = \Psi_6$ and $\Psi_5 = \Psi_7$. It can then be shown that $\sigma$ is co-axial with $B$ and that the three principal stresses are given by

$$\sigma_1 = 2\Psi_1\lambda_1^2 + 2\Psi_2(\lambda_1^2\lambda_2^2 + \lambda_1^2\lambda_3^2) + (4\Psi_4 + 2\Psi_8)\lambda_1^2\cos^2\phi + 8\Psi_5\lambda_1^4\cos^2\phi - p, \tag{2.11}$$

$$\sigma_2 = 2\Psi_1\lambda_2^2 + 2\Psi_2(\lambda_1^2\lambda_2^2 + \lambda_3^2\lambda_2^2) + (4\Psi_4 - 2\Psi_8)\lambda_2^2\sin^2\phi + 8\Psi_5\lambda_2^4\sin^2\phi - p, \tag{2.12}$$

$$\sigma_3 = 2\Psi_1\lambda_3^2 + 2\Psi_2(\lambda_1^2\lambda_3^2 + \lambda_2^2\lambda_3^2) - p. \tag{2.13}$$

Furthermore, we may define an effective strain-energy function $W(\lambda_1, \lambda_2, \lambda_3)$ through

$$W(\lambda_1, \lambda_2, \lambda_3) = \Psi(I_1, I_2, ..., I_8), \tag{2.14}$$

and show that

$$\sigma_i = \lambda_i W_i - p, \quad (\text{no summation on } i), \quad i = 1, 2, 3, \tag{2.15}$$

where $W_i = \partial W/\partial\lambda_i$. Thus, as far as axisymmetric deformations are concerned, the fibre-reinforced cylindrical tube behaves like a cylindrical tube made of an isotropic hyperelastic material with strain-energy function $W(\lambda_1, \lambda_2, \lambda_3)$. This in turn ensures that the assumed axisymmetric deformation can indeed be realized.

We now specialize the above formulation to the case when the deformation is a uniform inflation corresponding to an internal pressure $P$. We denote the deformed inner and outer radii by $a$ and $b$, respectively. With the condition of incompressibility taken into account, the deformation must necessarily take the form

$$r^2 = \lambda_z^{-1}(R^2 - A^2) + a^2, \quad \theta = \Theta, \quad z = \lambda_z Z, \tag{2.16}$$

where $\lambda_z$ is the stretch in the axial direction which is assumed to be a constant throughout this paper.

It can be shown [13] that in terms of the reduced strain-energy function $w(\lambda_1, \lambda_2)$ defined by

$$w(\lambda_1, \lambda_2) = W(\lambda_1, \lambda_2, (\lambda_1\lambda_2)^{-1}), \tag{2.17}$$

the internal pressure is given by

$$P = \int_{\lambda_b}^{\lambda_a} \frac{w_1}{\lambda^2\lambda_z - 1} d\lambda, \tag{2.18}$$

where $w_1 = \partial w/\partial\lambda$, and the two limits $\lambda_a$ and $\lambda_b$ are defined by

$$\lambda_a = \frac{a}{A}, \quad \lambda_b = \frac{b}{B},$$

and are related to each other by

$$\lambda_a^2\lambda_z - 1 = \frac{B^2}{A^2}(\lambda_b^2\lambda_z - 1). \tag{2.19}$$

The resultant axial force at any cross section is independent of $Z$ and is given by

$$F(\lambda_a,\lambda_z)\equiv 2\pi\int_a^b \sigma_{22}rdr-\pi a^2P=\pi A^2(\lambda_a^2\lambda_z-1)\int_{\lambda_b}^{\lambda_a}\frac{2\lambda_z w_2-\lambda w_1}{(\lambda^2\lambda_z-1)^2}\lambda d\lambda, \tag{2.20}$$

where $w_2=\partial w/\partial\lambda_z$. We have shown $F$ explicitly as a function of $\lambda_a$ and $\lambda_z$ (the $\lambda_b$ in the equation is eliminated using (2.19)). Likewise, the pressure defined by (2.18) is also viewed as a function of $\lambda_a$ and $\lambda_z$ in the subsequent analysis.

By considering an eigenvalue problem governing axisymmetric incremental deformations, it was shown in Fu *et al* [5], with the aid of the dynamical systems theory, that the bifurcation condition for the initiation of a localized bulge has the simple representation

$$\Omega(\lambda_a,\lambda_z)\equiv J(P,F)=0, \tag{2.21}$$

where the first equation defines the function $\Omega(\lambda_a,\lambda_z)$ and $J(P,F)$ is the Jacobian of $P$ and $F$ when both are viewed as functions of $\lambda_a$ and $\lambda_b$, that is,

$$J(P,F)=\frac{\partial P}{\partial\lambda_a}\frac{\partial F}{\partial\lambda_z}-\frac{\partial P}{\partial\lambda_z}\frac{\partial F}{\partial\lambda_a}. \tag{2.22}$$

Thus, the bifurcation condition $\Omega(\lambda_a,\lambda_z)=0$ has a clear physical meaning: it is satisfied when the Jacobian of $P$ and $F$ vanishes (or equivalently, $P=P(\lambda_a,\lambda_z)$ and $F=F(\lambda_a,\lambda_z)$ cannot locally be inverted to express $\lambda_a$ and $\lambda_z$ in terms of $P$ and $F$). It was also shown in Fu *et al* [5] that when $F$ is fixed, the initiation pressure for localized bulging is simply the maximum pressure in uniform inflation, but this correspondence is lost if it is the axial stretch $\lambda_z$ that is fixed. Finally, in the membrane limit $H/R_m\to 0$, where $H$ and $R_m$ denote the undeformed wall thickness and mean radius respectively, the pressure and axial force to leading order are given by

$$P=\frac{H}{R_m}\cdot\frac{w_1}{\lambda_a\lambda_z},\qquad \frac{F}{2\pi HR_m}=w_2-\frac{\lambda_a w_1}{2\lambda_z}, \tag{2.23}$$

and the bifurcation condition (2.21) reduces to

$$\Omega^{(0)}(\lambda_a,\lambda_z)\equiv\lambda_a(w_1-\lambda_z w_{12})^2+\lambda_z^2 w_{22}(w_1-\lambda_a w_{11})=0, \tag{2.24}$$

where $\lambda_a$ should now be interpreted as the circumferential stretch in the mid-surface. The above bifurcation condition has previously been derived with the use of membrane equilibrium equations; see, e.g., Fu *et al* [14].

## 3 Effects of bending stiffness and fibre-reinforcement

Once the strain-energy function is specified, the effects of bending stiffness (through the finite thickness) and fibre-reinforcement on the initiation of localized bulging can be assessed using the bifurcation condition (2.21). As an illustration, we consider the material model given by

$$\Psi=-\frac{1}{2}\mu J_m\log(1-\frac{I_1-3}{J_m})-\frac{1}{2}\mu k_1 J_f\sum_{\alpha=4,6}\log(1-\frac{(I_\alpha-3)^2}{J_f}), \tag{3.1}$$

where $\mu$ is the ground-state modulus, $k_1$ is a measure of the strength of fibre-reinforcement, whereas $J_m$ and $J_f$ measure the extensibility of the matrix material and reinforcing fibres, respectively. The first term in (3.1) for the matrix material is the well-known Gent material model [15]. The second term representing the

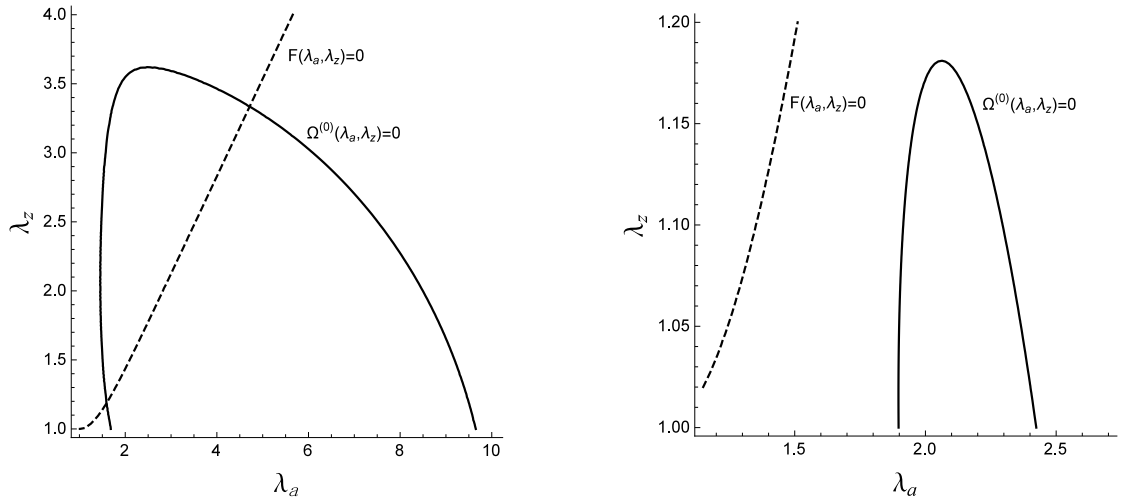


**Fig. 2** The contour plots of $\Omega^{(0)}(\lambda_a, \lambda_z) = 0$ and $F(\lambda_a, \lambda_z) = 0$ under the membrane assumption. (a): $k_1 = 0$; (b): $k_1 = 1/15$, $J_f = 30$, $\phi = 30^o$. They show the fact that without fibre-reinforcement localized bulging is possible if either the axial stretch or the axial force is fixed, but with fibre-reinforcement localized bulging is only possible if the axial stretch is fixed to be less than 1.18.

contribution of the reinforcing fibres was first suggested by Horgan & Saccomandi [16], and the particular combination in (3.1) was suggested by Ogden & Saccomandi [17] who also compared it with other material models.

Our subsequent discussion is independent of the shear modulus $\mu$ and so we do not need to specify its value. Without loss of generality, we take $B = 1$, or equivalently, we take $B$ to be the length unit against which all other lengths are measured. The effect of bending stiffness is then assessed by changing the value of the inner radius $A$. We shall assume that $J_m$ takes the fixed value of 97.2, as suggested by Gent [15], and investigate the effects of varying the other material parameters $\phi$, $k_1$ and $J_f$. As demonstrated in our earlier papers, see, e.g., Fu *et al* [5], a most transparent way to understand the initiation of localized bulging is by plotting the solution of the bifurcation condition $\Omega(\lambda_a, \lambda_z) = 0$ and the equation $F(\lambda_a, \lambda_z) = F_0$ together in the $(\lambda_a, \lambda_z)$-plane, where $F_0$ is a constant. This is achieved numerically in a straightforward manner with the aid of *Mathematica* [18]. The curve $F(\lambda_a, \lambda_z) = F_0$ is of course only relevant when the resultant axial force is fixed to be equal to $F_0$, in which case the curve represents the appropriate loading path in the $(\lambda_a, \lambda_z)$-plane. Localized bulging can occur only if the two curves have an intersection. On the other hand, when it is the axial stretch $\lambda_z$ that is fixed, the loading path is simply a horizontal line in the $(\lambda_a, \lambda_z)$-plane, and in this second case localized bulging can occur only if this line and $\Omega(\lambda_a, \lambda_z) = 0$ have an intersection.

We first consider the effects of fibre reinforcement under the membrane assumption. Fig.2 shows the two curves mentioned above in the $(\lambda_a, \lambda_z)$-plane with $F_0 = 0$. These effects have previously been examined in our earlier paper [2] and by Demirkoparan & Merodio [19] using different strain-energy functions. It is seen that when the axial force $F$ is fixed to be zero, localized bulging can occur when there is no fibre reinforcement, but it becomes impossible when fibre reinforcement is added. However, Fig.2(b) shows that localized bulging can still occur if the axial stretch $\lambda_z$ is fixed to be less than 1.18. This fact has previously been established in our earlier studies; see, e.g., Fu *et al* [2].

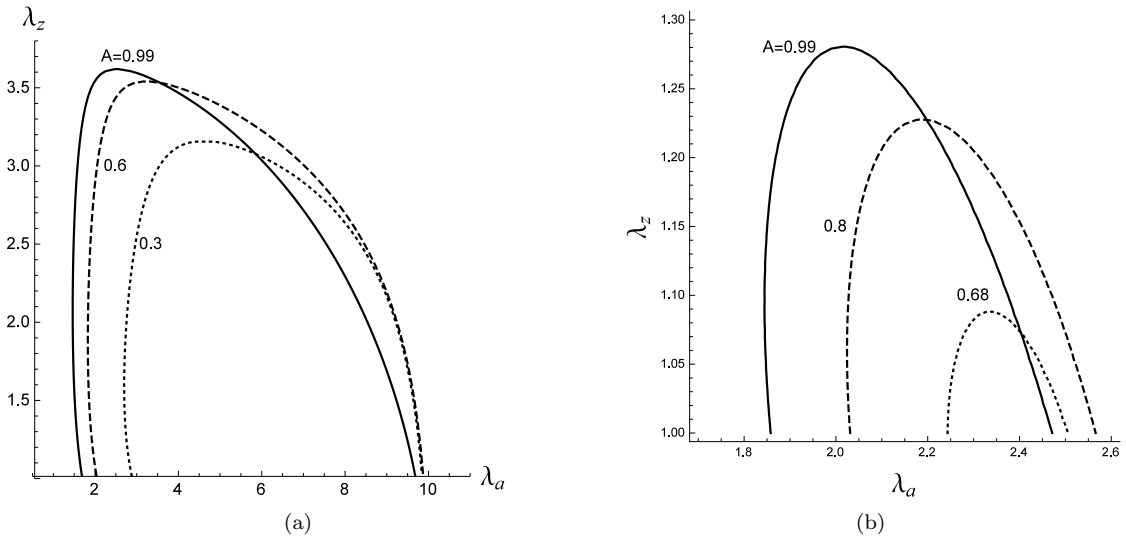


**Fig. 3** Plot of $\Omega(\lambda_a, \lambda_z) = 0$ for three representative values of $A$. (a): Without fibre-reinforcement; (b): with fibre-reinforcement ($k_1 = 1/20$, $J_f = 30$, $\phi = 30^o$). It shows the fact that with fibre-reinforcement the bifurcation curve moves down quickly as $A$ is decreased and the curve disappears completely at a threshold value of $A$.

Under the membrane assumption, the tube has no bending stiffness. It was shown in [5] that taking into account bending stiffness in the case of an isotropic hyperelastic tube has no qualitative effect on localized bulging and the membrane theory is capable of predicting the initiation pressure accurately for thickness /radius ratio $H/R_m$ as large as 0.67. This is illustrated in Fig.3(a) where it is shown that the bifurcation condition still has a solution when $A$ is as small as 0.3 (in fact for all values of $A$ although not shown). In contrast, Fig.3(b) shows that bending stiffness has a drastic effect on the initiation pressure when fibre-reinforcement is present. It is seen that as $A$ is reduced (that is, as the wall thickness is increased), the bifurcation curve moves down rapidly, and it disappears completely when $A$ becomes smaller than 0.65. Thus, for the particular set of material parameters indicated in the caption, localized bulging becomes impossible when $H/R_m$ becomes bigger than 0.42 whether it is the axial force or axial stretch that is fixed during inflation.

Fig.4 shows how the behaviour shown in Fig.3(b) depends on the parameter $k_1$, a measure of the volume fraction of fibre-reinforcement. It is seen that the behaviour is similar when different values of $k_1$ are used, but the larger the value of $k_1$ is, the earlier the bifurcation curve disappears. For instance, when $k_1 = 1/10$, the threshold value of $A$ is approximately 0.77, corresponding to a thickness/radius ratio as small as 0.26.

To illustrate the effects of pathological changes in human arteries, we may start with $A = 0.77, k_1 = 1/10, J_f = 30, \phi = 30^o$ for which localized bulging is impossible because the bifurcation condition does not have a solution. This set of values may be viewed as corresponding to a healthy artery, and pathological changes may be modeled by a reduction in the fibre volume, or equivalently in the value of $k_1$. As $k_1$ is reduced from 1/10, the bifurcation condition very quickly begins to have a solution. For instance, when $k_1$ is reduced to 1/11, the bifurcation condition has a solution whose graph lies just below $\lambda_z = 1.014$. This means that at this slightly reduced value of $k_1$ localized bulging becomes possible provided $\lambda_z < 1.014$.

The effect of varying the fibre extensibility $J_f$ is shown in Fig.5. It is seen that for each fixed value of $A$ the bifurcation curve also moves down rapidly when $J_f$ is reduced. For the particular set of material and geometrical parameters shown in the caption, the curve disappears when $J_f$ becomes smaller than 23.

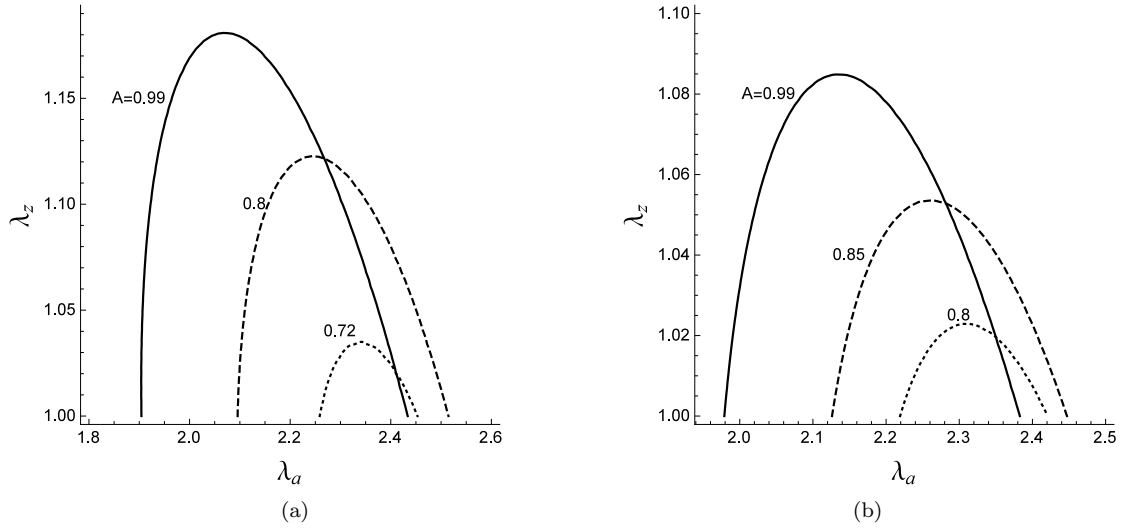


(a) (b)

**Fig. 4** Effects of finite thickness/bending stiffness for two different values of $k_1$ while $J_s$ and $\phi$ are fixed to be 30 and $30^o$, respectively. (a): $k_1 = 1/15$; (b): $k_1 = 1/10$. It is seen that the stronger the fibre-reinforcement, the earlier the bifurcation curve disappears as $A$ is decreased.

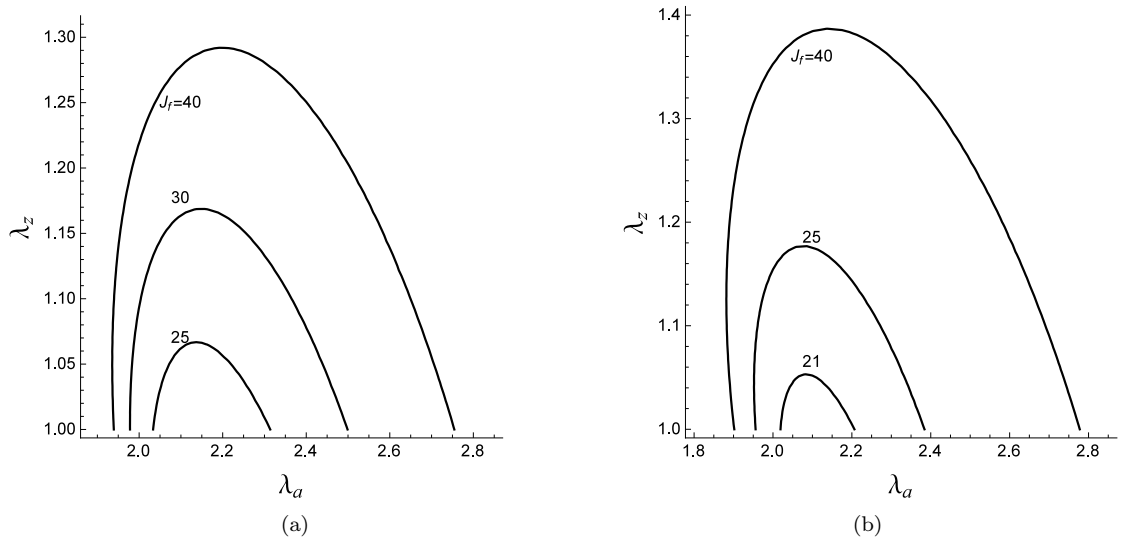


(a) (b)

**Fig. 5** Effects of fibre extensibility (characterized by $J_f$) with $A = 0.9$ and $\phi = 30^o$ fixed. (a): Solution of $\Omega(\lambda_a, \lambda_z) = 0$ with $k_1 = 1/15$; (b): solution of $\Omega(\lambda_a, \lambda_z) = 0$ with $k_1 = 1/20$.

Finally, the effect of changing the fibre orientation is shown in Fig.6(a, b). It is seen that as $\phi$ is increased from zero, the bifurcation curve goes down first until $\phi$ reaches approximately $30^o$ after which the curve goes up and spreads out in the $\lambda_a$-direction. Thus, there exists an optimal angle at which localized bulging becomes most unlikely.

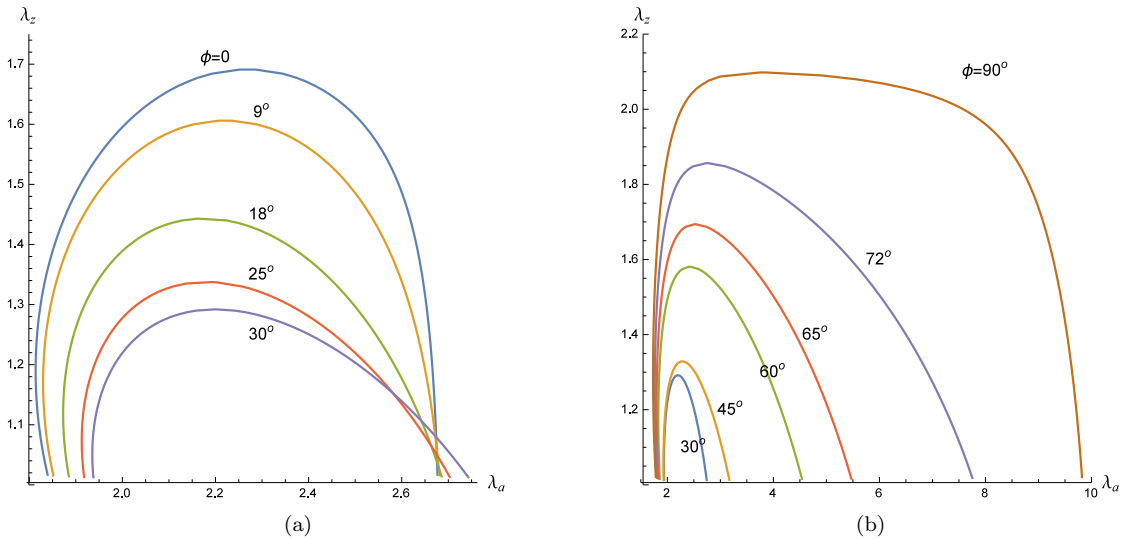


**Fig. 6** Effects of fibre orientation $\phi$ with $A = 0.9$, $k_1 = 1/15$ and $J_f = 40$ fixed. All the curves are the solutions of $\Omega(\lambda_a, \lambda_z) = 0$ for the values of $\phi$ indicated.

## 4 Conclusion

This paper has focussed on the effects of fibre-reinforcement on localized bulging in an inflated cylindrical tube of arbitrary thickness. It extends a recent study, Fu *et al* [5], that examined the effects of bending stiffness for an isotropic cylindrical tube without fibre-reinforcement. Our study has been facilitated by the fact that with fibre-reinforcement symmetric with respect to the axis of the cylinder, see Fig.1, the tube under inflation behaves effectively like an isotropic tube with material constants representing fibre-reinforcement appearing as passive parameters in the analysis. Thus, the bifurcation condition derived in [5] can be applied after appropriate modifications. We have used a representative strain-energy function to illustrate the combined effects of bending stiffness, amount of fibre-reinforcement, fibre extensibility, and fibre orientation. It is shown that localized bulging can be eliminated completely, irrespective of the end conditions, if the bending stiffness or the amount of fibre-reinforcement is sufficiently large, or fibre extensibility is sufficiently small. In contrast, the effect of fibre orientation is not monotonic, and there exists an optimal angle at which localized bulging is most unlikely to occur if all the other parameters are fixed. In any application where localized bulging is to be prevented, e.g., in the design of the Anaconda wave energy extraction device, optimization subject to certain constraint conditions will probably be required, but the necessary ingredients for such optimization are given in the current paper. Our findings support the view that aneurysms cannot occur in healthy arteries because of their optimal design through fibre-reinforcement and appropriate thickness, but may become possible as a mechanical bifurcation phenomenon under pathological changes. Our current study also provides a good starting point from which other material models and multi-layered or functionally graded tubes can be studied.

Acknowledgements

This work was supported by the National Natural Science Foundation of China (Grant Nos 11526141 and 11372212).

## References


1. A. Mallock, Note on the instability of india-rubber tubes and balloons when distended by fluid pressure. *Proc. Roy. Soc.*, A 49, 458-463 (1891).
2. Y.B. Fu, G. A. Rogerson, and Y.T. Zhang, Initiation of aneurysms as a mechanical bifurcation phenomenon. *Int. J. Non-linear Mech.*, 47, 179-184 (2012).
3. Y.B. Fu, and A.T. Il'chev, Localized standing waves in a hyperelastic membrane tube and their stabilization by a mean flow. *Maths Mech. Solids*, 20, 1198-1214 (2015).
4. A. Bucchi and G.E. Hearn, Delay or removal of aneurysm formation in the anaconda wave energy extraction device. *Renewable Energy*, 55, 104-119 (2013).
5. Y.B. Fu, J.L. Liu and G.S. Francisco, Localized bulging in an inflated cylindrical tube of arbitrary thickness the effect of bending stiffness. *J. Mech. Phys. Solids*, 90, 45-60 (2016).
6. H. Alexander, Tensile instability of initially spherical balloons. *Int. J. Eng. Sci.*, 9, 151-160 (1971).
7. R. Benedict, A. Wineman and W.H. Yang, The determination of limiting pressure in simultaneous elongation and inflation of nonlinear elastic tubes. *Int. J. Solids Struct.*, 15, 241-249 (1979).
8. M.M. Caroll, Pressure maximum behaviour in inflation of incompressible elastic hollow spheres and cylinders. *Quart. of Appl. Math.*, 45, 141-154 (1987).
9. L.M. Kanner and C.O. Horgan, Elastic instabilities for strain-stiffening rubber-like spherical and cylindrical thin shells under inflation. *Int. J. Non-linear Mech.*, 42, 204-215 (2007).
10. L. Horny, M. Netusil and Z. Horak, Limit point instability in pressurization of anisotropic finitely extensible hyperelastic thin-walled tube. *Int. J. Non-Linear Mech.*, 77, 107-114 (2015).
11. J.-S. Ren, J.-W. Zou and X.-G., Yuan, Instability analysis in pressurized three-layered fiber-reinforced anisotropic rubber tubes in torsion. *Int. J. Eng. Sci.*, 49, 342-353 (2011).
12. A.J.M. Spencer, Constitutive theory for strongly anisotropic solids, in: A.J.M. Spencer (ed.), Continuum Theory of the Mechanics of Fibre-reinforced Composites, CISM Courses and Lectures No. 282, Springer-Verlag, Wien, 1984, pp 1-32.
13. D.M. Haughton and R.W. Ogden, Bifurcation of inflated circular cylinders of elastic material under axial loading ii. exact theory for thick-walled tubes. *J. Mech. Phy. Solids*, 27, 489-512 (1979).
14. Y.B. Fu, S.P. Pearce and K.-K. Liu, Post-bifurcation analysis of a thin-walled hyperelastic tube under inflation. *Int. J. Non-linear Mech.*, 43, 697-706 (2008).
15. A. Gent, A new constitutive relation for rubber. *Rubber Chem. Technol.*, 69, 59-61 (1996).
16. C.O. Horgan and G. Saccomandi, A new constitutive theory for fibre-reinforced incompressible non-linearly elastic solids. *J. Mech. Phy. Solids*, 53, 1985-2015 (2005).
17. R.W. Ogden and G. Saccomandi, Introducing mesoscopic information into constitu- tive equations for arterial walls. *Biomechan. Model. Mechanobiol.*, 6, 333-344 (2007).
18. S. Wolfram, Mathematica: A System for Doing Mathematics by Computer (2nd Edn). Addison-Wesley, California (1991).
19. H. Demirkoparan and J. Merodio, Bulging bifurcation of inflated circular cylinders of doubly fiber-reinforced hyperelastic material under axial loading and swelling. *Math. Mech. Solids*, DOI: 10.1177/1081286515600045 (2015).